Chapter 2

Verification of the Grisham Algorithm

2.1 Overview

No example problems or specific results were published by Grisham [6] to validate the algorithm he presented. In order to verify the results of the current implementation, an example is taken from *Analysis and Design of Flight Vehicle Structures* [8] and the results are compared to the Grisham algorithm prediction.

2.2 Example problem

This example is a shear beam with 6 panels, schematically depicted in Figure 2.1, having the following dimensions:

1. $l = 1524$ mm (60 in)
2. $h = 762$ mm (30 in)
3. $h_e = 748$ mm (29.45 in)
4. $h_c = 725.4$ mm (28.56 in)
5. $d = 254$ mm (10 in)
6. $t = 0.635$ mm (0.025 in)
7. $A_{fl} = 243.9$ mm^2 (0.378 in^2)
8. $A_{fu} = 435.5$ mm^2 (0.675 in^2)
9. $A_u = 151.2$ mm^2 (0.253 in^2)

The web material is 2024-T3 aluminum sheet with the following material properties:

1. $\sigma_{yt} = 289$ MPa (42 ksi)

2. $\sigma_{ut} = 441$ MPa (64 ksi)
3. $E_w = 72.4$ GPa (10 500 ksi)

The two flanges are fabricated from 7075-T6 aluminium alloy extrusions, with the following material properties:

1. $\sigma_{yt} = 483$ MPa (70 ksi)
2. $\sigma_{ut} = 538$ MPa (78 ksi)
3. $E_f = 71.0$ GPa (10 300 ksi)

The uprights are fabricated from 2014-T6 aluminium alloy extrusions, with the following material properties:

1. $\sigma_{yt} = 366$ MPa (53 ksi)
2. $\sigma_{ut} = 414$ MPa (60 ksi)
3. $E_u = 72.4$ GPa (10 500 ksi)

Both flanges have a T-shaped cross-section. The uprights are angles (25.4 mm $\times$ 25.4 mm $\times$ 3.175 mm or 1 in $\times$ 1 in $\times$ $\frac{1}{8}$ in) and are made from 2014-T6 alloy. The shear load applied to the beam is $P = 60\ 048$ N (13 500 lb).

In this example two different methods are followed to solve the problem, namely the modified Wagner equations based on [1, 2] and the NACA approach [3, 4]. The results of both these approaches are compared to the current implementation of the Grisham algorithm. The various assumptions and limitations of the two methods are discussed below.

The modified Wagner approach incorporates:

1. The shear strength of the beam flanges.
2. The shear carried by the web before the onset of buckling.

The remainder of the shear in the beam after subtracting the components listed in (1) and (2) above is considered to be carried by the web in a buckled state in the form of a diagonal tension field.

The NACA approach is to be used subject to the following restrictions:

1. The uprights on the web stiffeners should not be too thin; the ratio of the stiffener thickness to web thickness should be greater than 0.6; i.e. $\frac{t_u}{t} > 0.6$.
2. The upright or web stiffener spacing shall not be outside the range $0.2 < \frac{d}{h} < 1.0$.

The NACA tests excluded very thin or very thick webs; non-conservative predictions may occur if $\frac{h}{t} > 1500$ or if $\frac{h}{t} < 200$.

Since:

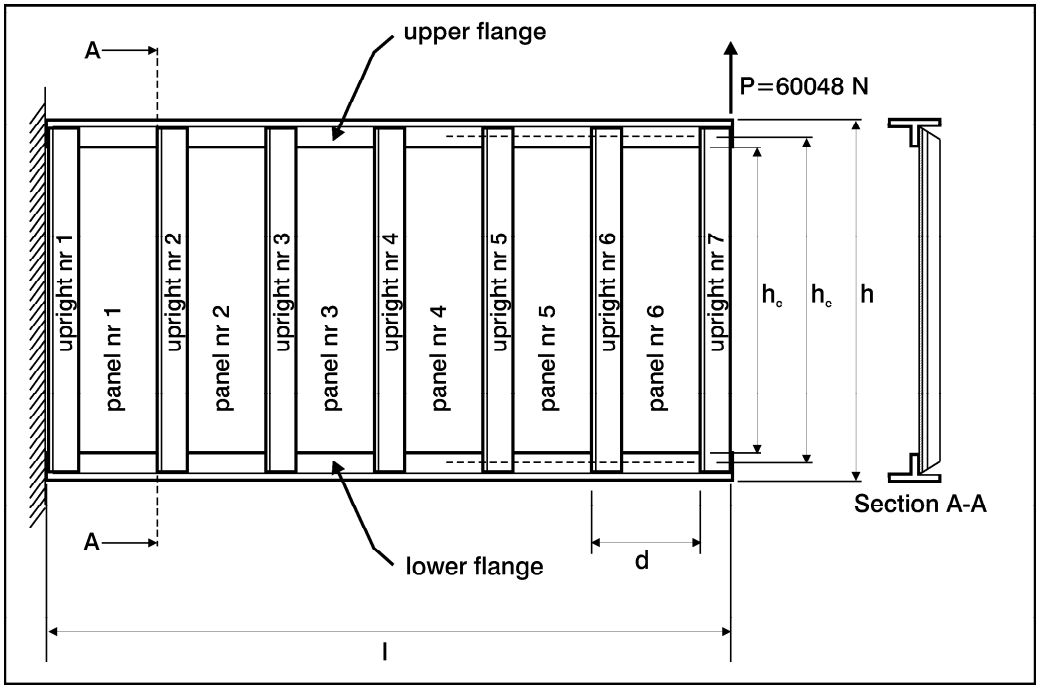

Figure 2.1: Layout of the cantilever beam used in the example

1. $\frac{t_u}{t} = 5.0$
2. $\frac{d}{h} = 0.33$
3. $\frac{h}{t} = 1142$

the use of the NACA equations is acceptable for the example under consideration.

(It should also be noted that, strictly speaking, the empirical relations developed by the NACA only apply to structures fabricated from 7076-T6 and 2024-T3 alloy since these were the only materials used in the NACA's extensive testing program.)

2.2.1 The finite element model

For the linear finite element analysis used in the Grisham algorithm, the flanges are modelled using second order beam elements, having a T-shaped cross-section. The uprights are also modelled with second order beam elements, having L-shaped cross-sections and their eccentricity is accounted for. The thin web is modelled with second order, isoparametric, thin shell elements having eight nodes per element. Small displacement theory is used. The shear load is applied vertically and distributed along all the nodes at the end of the beam. The ABAQUS® commercial finite element package is used for the linear finite element analysis. (It is also used for all subsequent finite element analyses in this thesis.) Plasticity effects are not taken into account and buckling of the uprights is also not considered. All four edges of the web are assumed to be simply supported when calculating the critical shear and

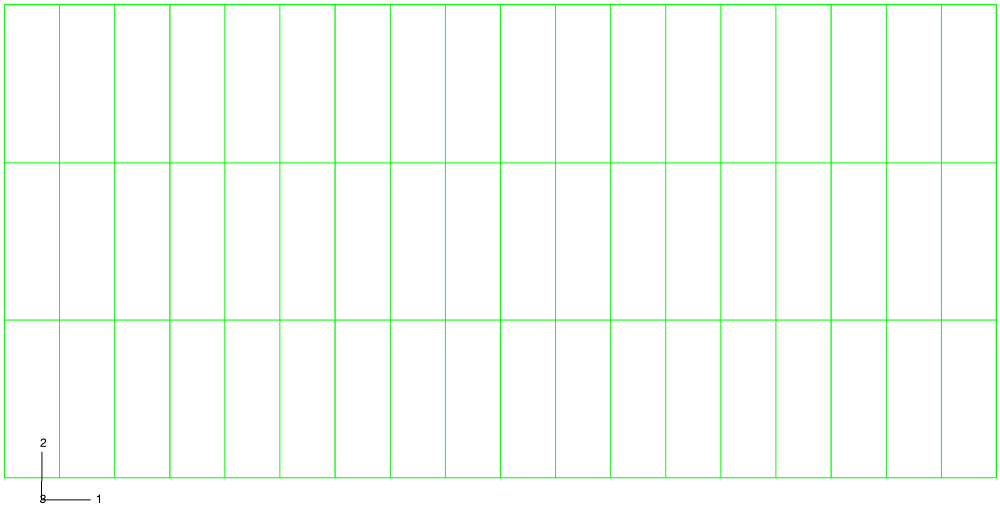

Figure 2.2: Finite element mesh for the verification example

compression buckling coefficients, as is done in the example in Bruhn [8]. Figure 2.2 shows the finite element mesh of the beam used to evaluate the Grisham algorithm. A coarse 3 × 3 mesh is used for the web of each panel.

2.2.2 Web results

In Table 2.1, the results for the panels obtained using the iterative procedure of Grisham are compared with results from the Wagner and NACA approaches. The four variables compared in the table are:

1. k - the diagonal tension factor. It indicates the degree to which the diagonal tension is developed and is defined as $\tau_{DT} = k\tau_{xy}$. When $k = 0$, no diagonal tension is present. When $k = 1$, the web is in pure diagonal tension.

2. α - the diagonal tension angle. In pure diagonal tension (PDT) this is the angle of the major principal stress relative to the horizontal for this example. In incomplete diagonal tension (IDT), it is the angle that the major principal stress would have if the sheet were not carrying part of the load in pure shear.

3. τ_{xy} - the shear stress in the web.

4. τ_{cr} - the critical web shear buckling stress. This is the stress at the onset of shear buckling.

	Grisham algorithm				Modified	
	Panel 2	Panel 3	Panel 4	Panel 5	Wagner	NACA [3, 4]
k	0.649	0.673	0.673	0.635	—	0.690
α [degrees]	42.1	42.0	42.0	42.2	43.0	41.3
τ_{xy} [MPa]	126.9	127.3	127.2	127.3	130.4	135.1
τ_{cr} [MPa]	2.624	2.624	2.624	2.624	2.358	2.551

Table 2.1: Comparison between Grisham algorithm, modified Wagner equations, and NACA approach

The results of panels 1 and 6 are ignored since they include edge effects that are automatically included via the finite element analysis and which are not accounted for in the NACA or Wagner approaches. Only five iterations are required for the Grisham results; this means that the system equations are solved only five times, while the stiffness matrix remains constant throughout (since the analyses are linear, simple superposition principles can be applied).

The results for the four panels obtained with the Grisham algorithm are very similar and compare closely to those of the other two methods. The value of the diagonal tension factor k from the Grisham algorithm is slightly lower than that of the NACA method. The diagonal tension factor k indicates the percentage of the total load that is carried in diagonal tension by the web. The value of $k = 0.69$ using the NACA methodology indicates that 69 % of the total load carried by the web is carried in diagonal tension and the rest in normal shear. The Grisham algorithm takes compression-compression buckling in both directions into account through an interaction equation which has an effect on the magnitude of the diagonal tension. In the NACA method this is not taken into account, resulting in conservative predictions. *When neglecting this effect of compression-compression buckling in Grisham's method, the NACA result of* $k = 0.69$ *is obtained exactly.*

The critical shear stress τ_{cr} (shear stress at the onset of buckling) for the Grisham algorithm and Wagner approach are based on analytical relations that depend on geometry and material properties. The NACA critical shear stress τ_{cr} includes empirical data in its calculation, relating to the stiffness of the flanges and uprights. The large difference between the critical shear stress value τ_{cr} and the total web shear stress shows that the final stress carried by the web is almost 50× higher than the initial buckling shear stress. The low value of τ_{cr} is a result of the relatively thin plate ($t = 0.635$ mm).

Table 2.2 gives the diagonal tension stress values as well as the compression buckling stresses of the web for each panel. The Modified Wagner and NACA methods do not produce values that can be compared to these and are therefore not included in Table 2.2. The final compressive stress values are very low. This indicates that the compressive-compressive buckling effects are not significant in this example. Figures 2.3, 2.4 and 2.5 show the stress results in the web from the Grisham algorithm's finite element analysis. The shear stress plot compares well to the results in Table 2.1. Figures 2.6 and 2.7 show vector plots of the maximum and minimum principal stresses in the web. The magnitudes of the stress values are very high for the web. In the worked example the intricacies of the finite element

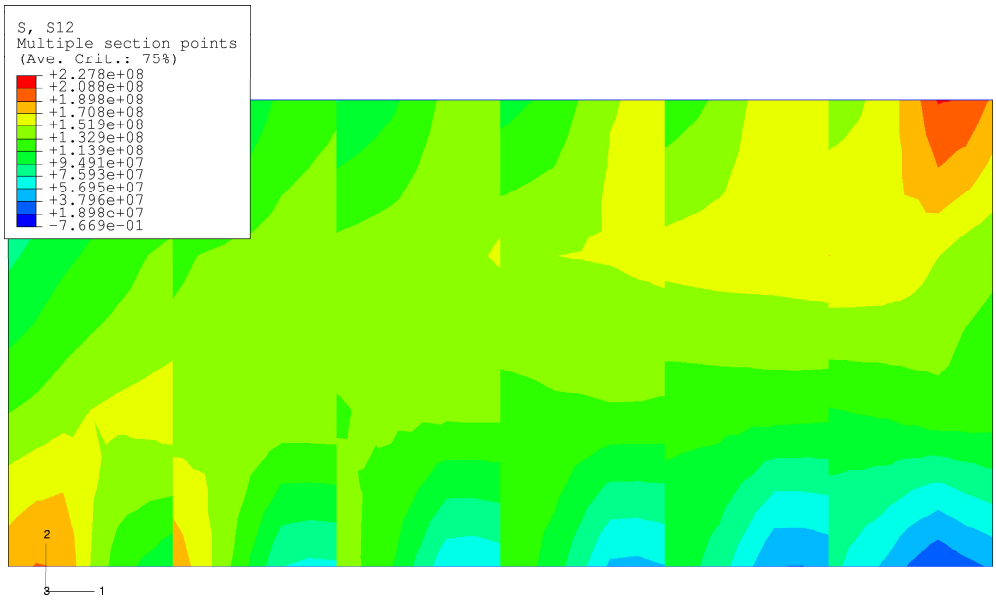

Figure 2.3: Unsmoothed shear stress distribution (τ_{xy}) in the web after the final iteration

method are not taken into account. Boundary conditions, having a localized effect are also not considered.

	Grisham algorithm			
	Panel 2	Panel 3	Panel 4	Panel 5
$\sigma_{x_{DT}}$ [MPa]	91.19	95.17	95.20	89.37
$\sigma_{y_{DT}}$ [MPa]	74.47	77.17	77.18	73.28
σ_{x_c} [MPa]	-0.473	-0.250	0.047	0.518
σ_{y_c} [MPa]	0.149	0.382	0.364	0.466

Table 2.2: Diagonal tension and compressive stress values calculated by means of the Grisham algorithm

2.2.3 Upright results

The results for the upright stresses are plotted in Figures 2.9 to 2.11. Values are plotted along the length of the upright at three different section points on the cross-section of the upright. Uprights number 1 and 7 are not considered because of boundary conditions. Figure 2.8 shows the position of these section points on the cross-section of the upright.

From the data in Figures 2.9 to 2.11 it can be seen that for all the uprights, the values at section points 5 and 9 are negative and therefore in compression while the values at

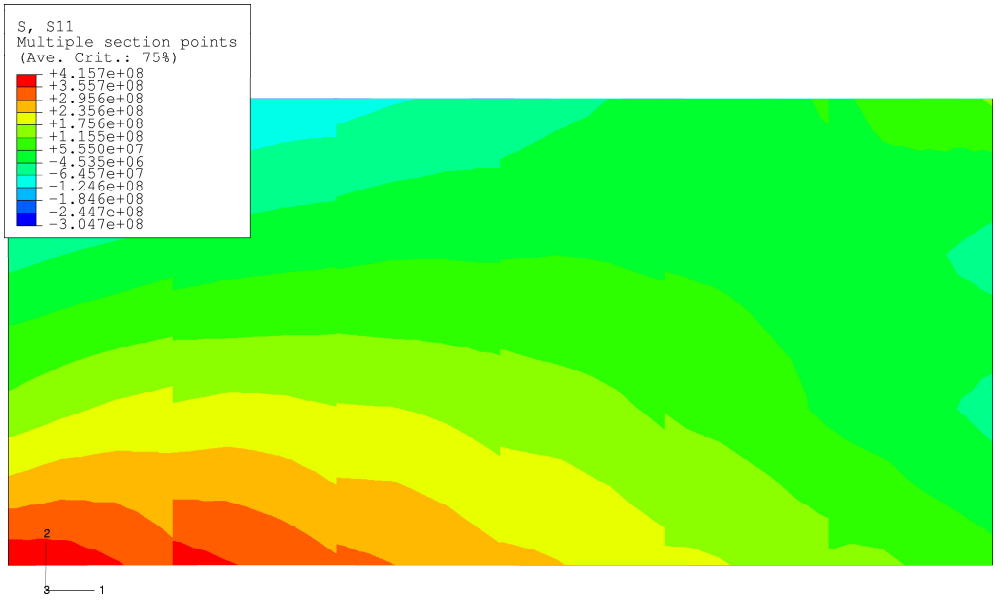

Figure 2.4: Unsmoothed normal stress (σ_x) in the web after the final iteration

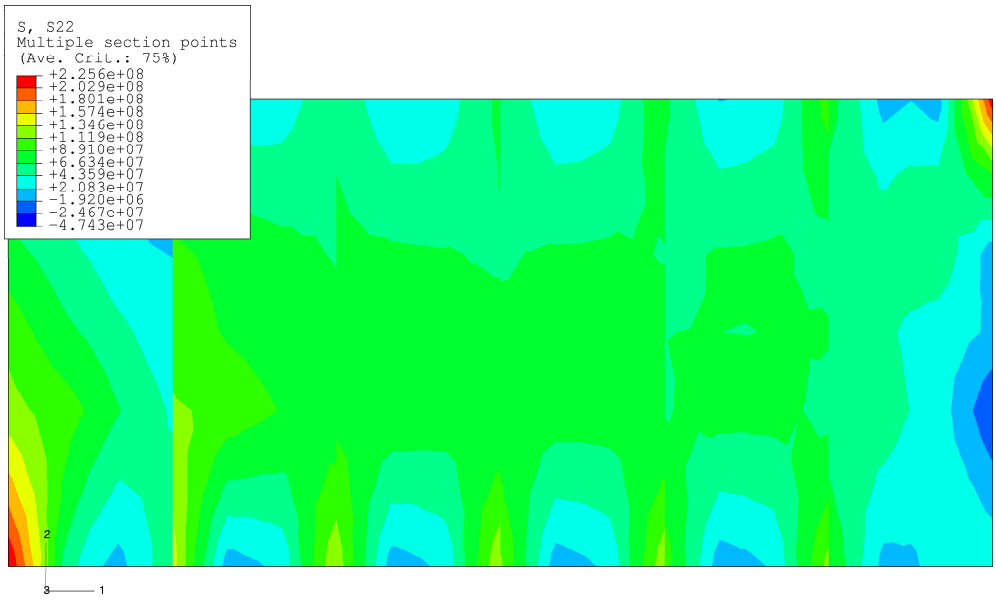

Figure 2.5: Unsmoothed normal stress (σ_y) in the web after the final iteration

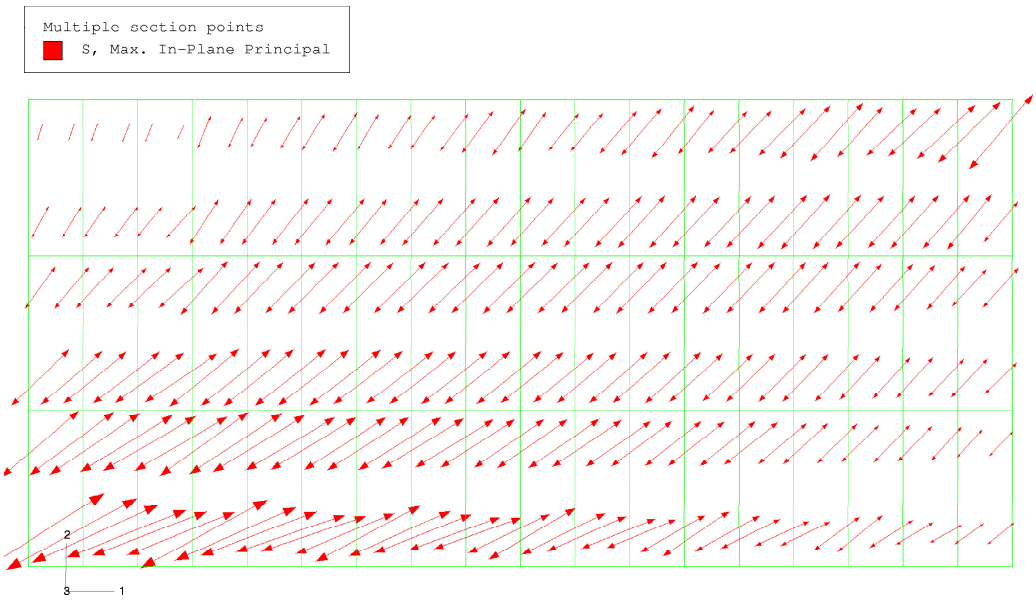

Figure 2.6: Maximum principal web stress vector plot after the final iteration

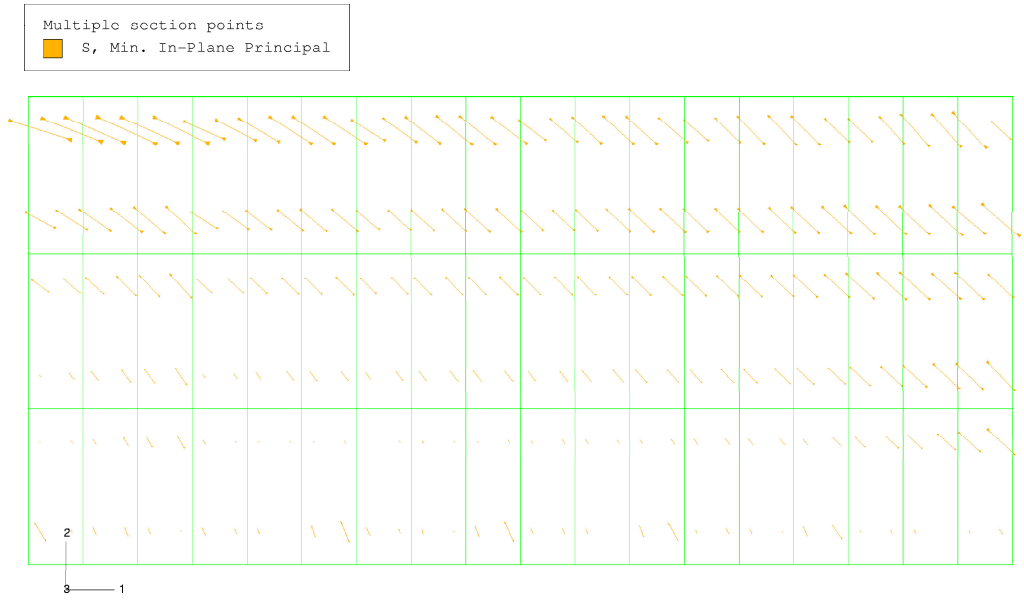

Figure 2.7: Minimum principal web stress vector plot after the final iteration

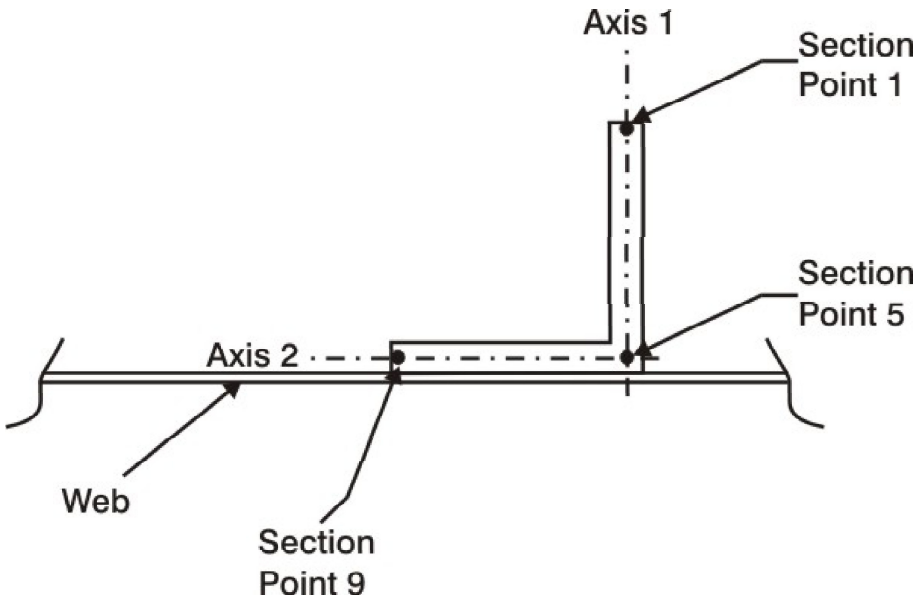

Figure 2.8: Cross-section of the upright showing the location of the section points

section point 1 are positive and therefore in tension. The upright behaves as a column loaded eccentrically along the median plane of the web by diagonal tension effects in the web. Although this tends to pull the two flanges together, creating a compressive load in the upright, it also causes bending due to the eccentricity and therefore the compressive stress tends to decrease in the upright when moving away from the web plane (towards section point 1). If the upright were symmetrical about the median plane of the web, the stresses would be compressive at all section points. The NACA equations predict that the maximum stress occurs in the upright at a point that coincides with the neutral axis of the beam. The upright stress then reduces in magnitude (parabolically) until the minimum upright stress is found at the two ends that are attached to the two flanges (known as the "gusset effect"). The neutral axis of the beam in this example is slightly above the centroid of the upright. At very high loading ratios ($\frac{\tau_{xy}}{\tau_{cr}} \gg 1$), such as in this example, the parabolic profile flattens out and all the stresses along the length of the upright are similar in magnitude.

Table 2.3 compares the results from the NACA method and that of the Wagner approach with the Grisham results. The average stress values are calculated along the length of the upright, using all the integration point values at section points 5 and 9. To compensate for eccentric loading the NACA method uses an effective area and only calculates average stresses at the median plane of the web. Section points 5 and 9 are closest to the median plane of the web. Wagner assumes that the uprights are like columns with elastic supports; that the web tension prevents the uprights from buckling out of the plane and that the total cross-section of the upright is in compression.

The average upright stress values of the Grisham algorithm are lower than that predicted by the NACA and Wagner approach. The stress magnitude in the upright is a direct indication of the magnitude of diagonal tension in the web. Since the diagonal tension factor for the Grisham algorithm is slightly lower than that predicted by the above mentioned methods,

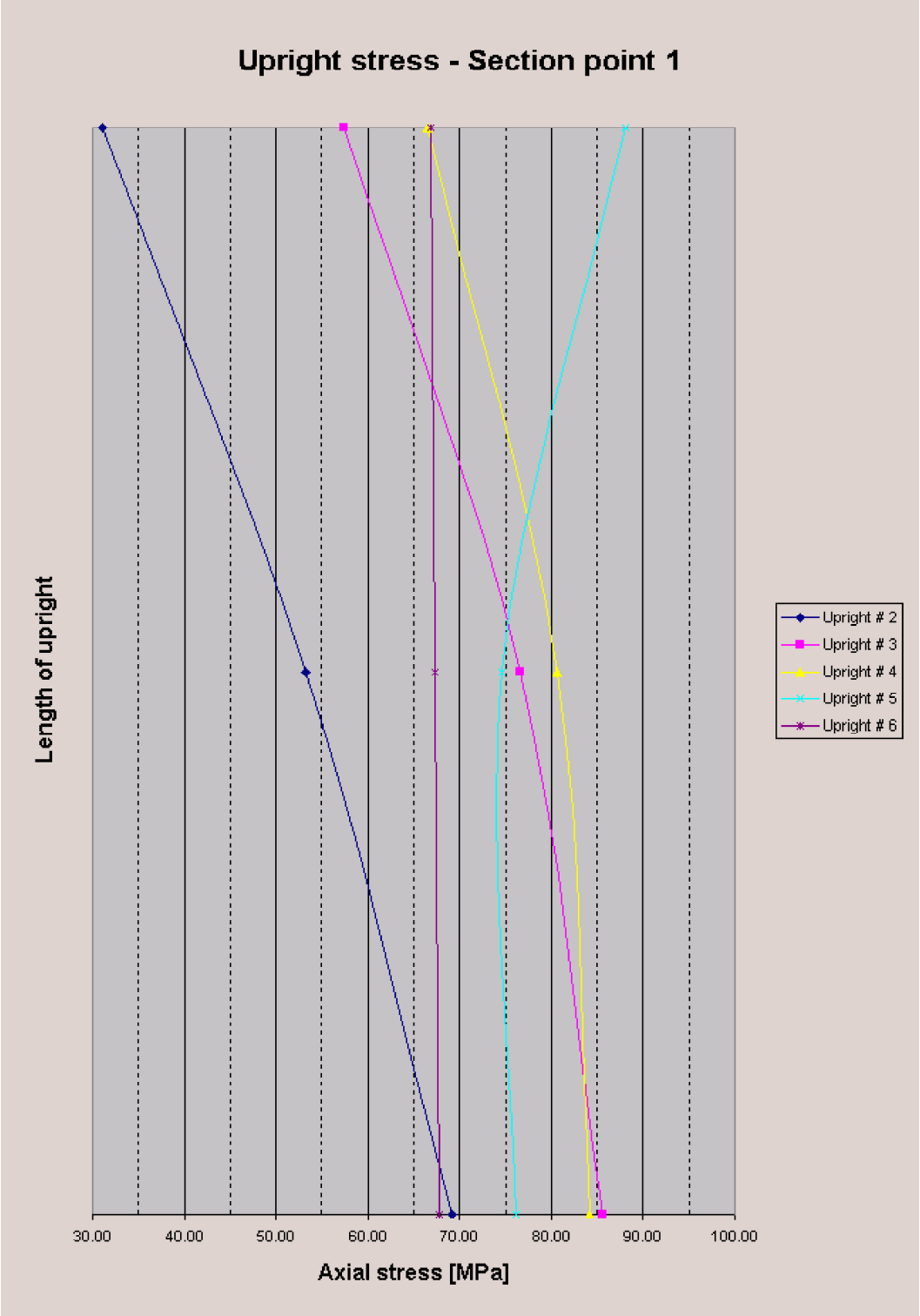

Figure 2.9: Axial stress along the length of the upright (σ_u) at section point 1

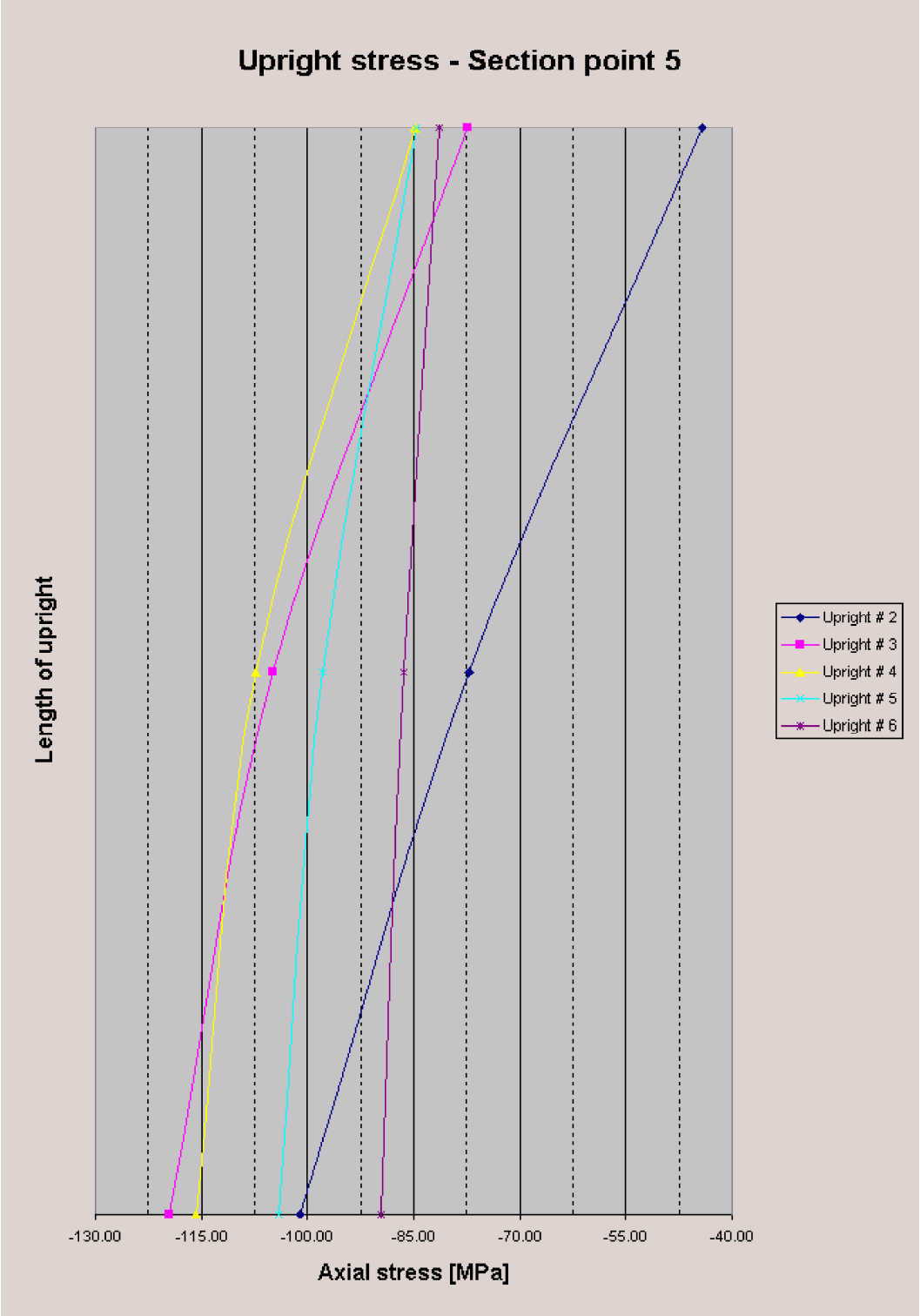

Figure 2.10: Axial stress along the length of the upright (σ_u) at section point 5

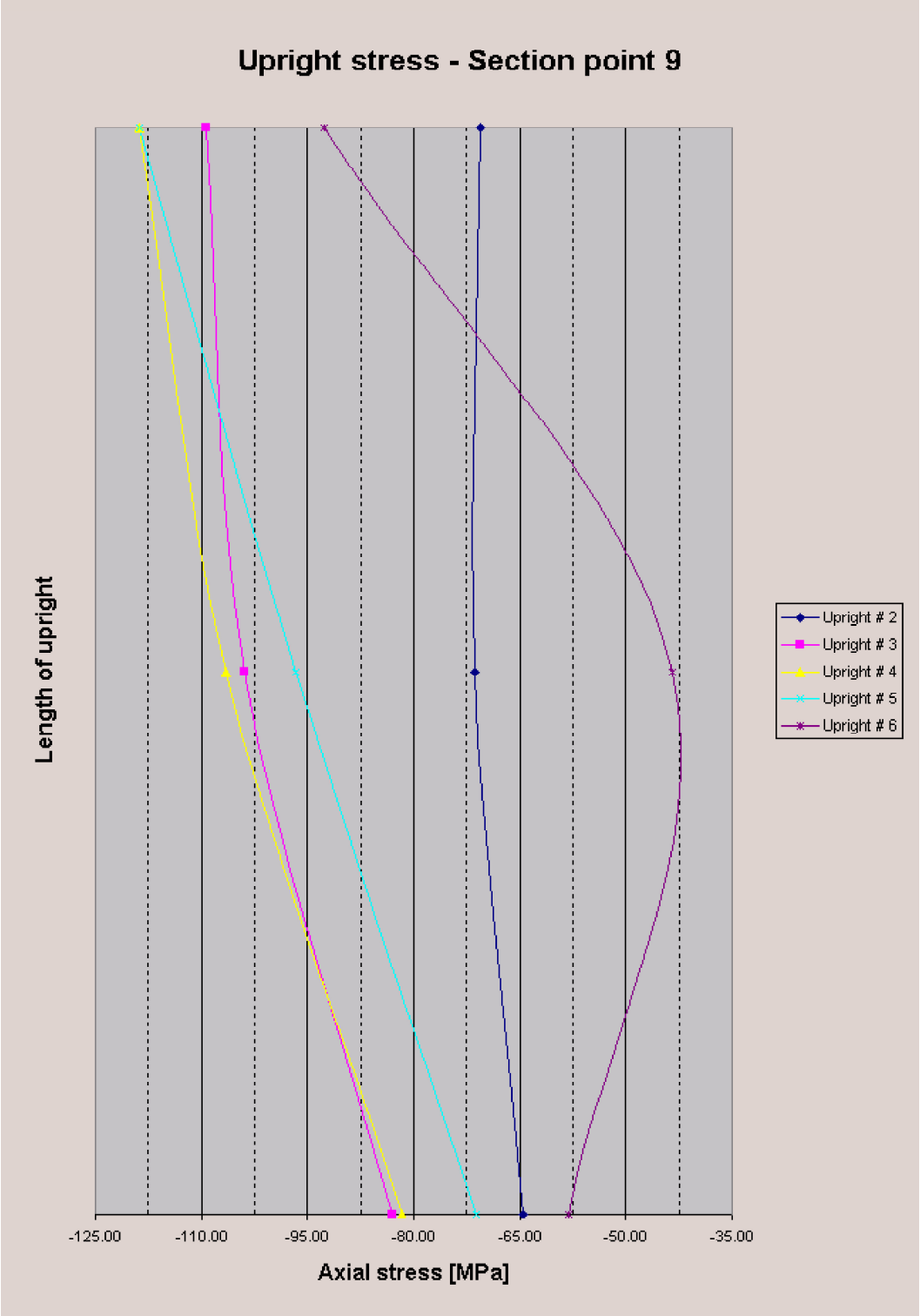

Figure 2.11: Axial stress along the length of the upright (σ_u) at section point 9

	Grisham algorithm					Modified	
	Upright 2	Upright 3	Upright 4	Upright 5	Upright 6	Wagner	NACA
$\overline{\sigma}_u$[MPa]	-71.4	-99.7	-102.4	-95.5	-75.3	-123.6	-116.5
$\sigma_{u_{max}}$[MPa]	-101.2	-119.7	-118.7	-118.7	-92.8	-123.6	-136.5

Table 2.3: Upright stress results

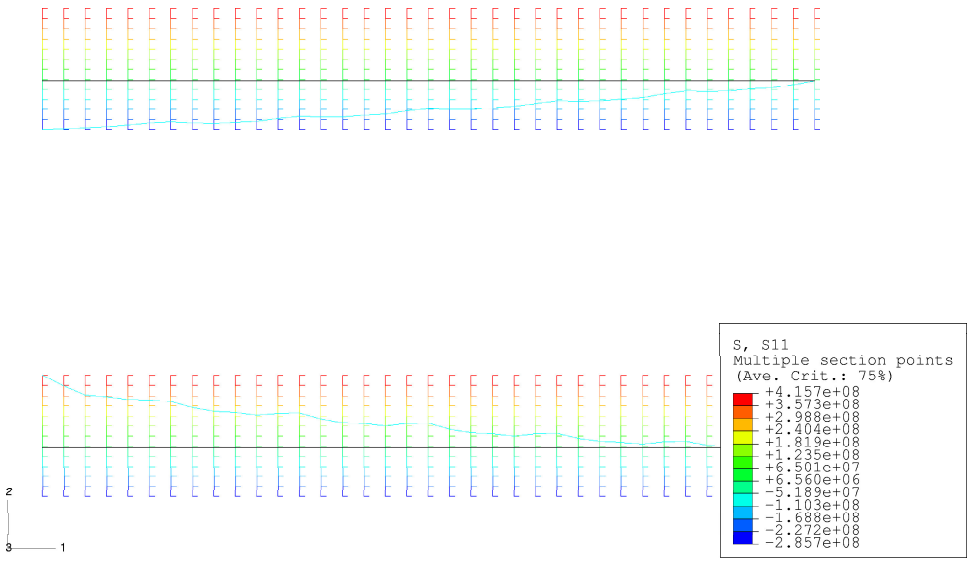

Figure 2.12: Axial stress distribution in the flanges after the final iteration of the Grisham algorithm

the upright stresses for the Grisham algorithm would also be lower.

2.2.4 Flange results

A contour plot of the axial stress distribution in the upper and lower flanges after the final iteration of the Grisham algorithm is shown in Figure 2.12. The flange stress values as calculated at section A-A in Figure 2.1 are given in Table 2.4. In the upper flange (compression flange), the high values of σ_{f_u} = -545.0 MPa and σ_{f_u} = -467.2 MPa are due to the secondary bending effects caused by diagonal tension in the web. Likewise in the lower flange (tension flange), the compressive values of σ_{f_l} = -427.0 MPa and σ_{f_l} = -288.4 MPa are also due to secondary bending effects caused by diagonal tension in the web. In a real life design situation both flanges would have to be redesigned because these values either exceed the yield stress of the material or are too close to the crippling stress [8] of $\sigma_{f_{cpl}}$ = -434.4 MPa.

The stress values for the Modified Wagner method as well as the NACA method can be split into three components: (i) the bending stress due to the applied shear load, (ii) the axial stress due to diagonal tension, and (iii) secondary bending stress due to diagonal tension. According to Kuhn [9] the calculation of the secondary bending stresses is conservative and can usually be neglected in practice. The flange stresses without the secondary bending stresses are given in Table 2.5. All lower flange stresses are now in tension and the values are also in much better agreement with those of the Grisham algorithm.

	Grisham Algorithm	Modified Wagner	NACA
σ_{f_u} [MPa] (upper fibre)	-216.9	-242.0	-237.2
σ_{f_u} [MPa] (lower fibre)	-255.0	-545.0	-467.2
σ_{f_l} [MPa] (upper fibre)	162.9	-427.0	-288.4
σ_{f_l} [MPa] (lower fibre)	275.2	460.0	408.4

Table 2.4: Flange stress results

	Grisham Algorithm	Modified Wagner	NACA
σ_{f_u} [MPa] (upper fibre)	-216.9	-312.3	-292.7
σ_{f_u} [MPa] (lower fibre)	-255.0	-304.5	-276.2
σ_{f_l} [MPa] (upper fibre)	162.9	292.4	281.0
σ_{f_l} [MPa] (lower fibre)	275.2	294.5	276.7

Table 2.5: Flange stress results excluding secondary bending effects

According to Peery [10] the stresses in the uprights and flanges may be five times less than that predicted by the theory of pure diagonal tension. The results predicted by Grisham are certainly less conservative, making it a more attractive method to use.

2.2.5 Deflection results

For the sake of completeness the displaced shape of the beam at the end of the iterative analysis is shown in Figure 2.13.

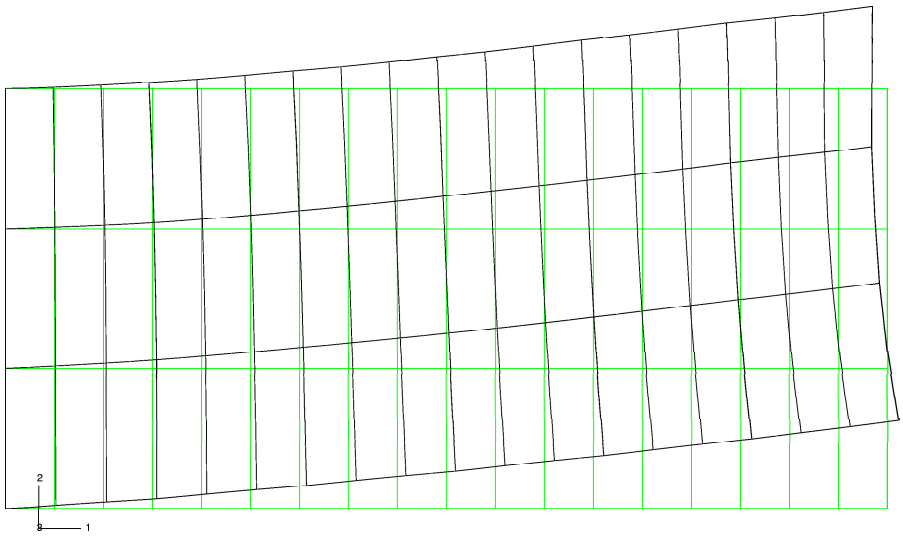

Figure 2.13: Displaced shape of the finite element model after the final iteration (undeformed shape in green)